



# A practical method for the estimation of directional wave spectra in reflective wave fields

Mark A. Davidson<sup>a,\*</sup>, David A. Huntley<sup>a</sup>, Paul A.D. Bird<sup>b</sup>

<sup>a</sup> *Institute of Marine Studies, Univ. of Plymouth, Drake Circus, Plymouth, Devon, PL4 8AA, UK*

<sup>b</sup> *School of Civil and Structural Eng., Univ. of Plymouth, Palace St., Plymouth, Devon, UK*

Received 19 August 1997; revised 12 December 1997; accepted 24 December 1997

---

## Abstract

A practical method is presented for the computation of directional spectra in presence of phase locked reflections (e.g., close to coastal structures). Existing modified directional analysis methods (e.g., The Modified Bayesian Method and the Modified Maximum Likelihood Method MMLM) require an input of the effective reflection line distance. In practice the position of the reflection line is often ambiguous leading to large errors in the directional spectrum. This paper presents a refinement of Isobe and Kondo's MMLM [Isobe, Kondo, K., 1984. Methods for estimating directional wave spectrum in incident and reflected wave field. Proc. 19th Conf. on Coastal Eng., Am. Soc. of Civil Eng., New York, pp. 467–483] which includes the reflection line position as an additional free parameter. The method presented here is based on minimising an error function which characterises the difference between the predicted and observed surface elevation variance observed at a number of spatially separated gauges. The new method is tested rigorously with both synthetic time-series and field data. Results indicate that the method is robust in a variety of incident wave conditions, in the presence of added noise and with only four transducers, providing the array is in close proximity to the shore. The new method of directional analysis when applied to field data produced frequency dependent reflection estimates which compared closely to those obtained by using the 2-dimensional approach of Gaillard et al. (1980) [Gaillard, P., Gauthier, M., Holly, F., 1980. Method of analysis of random wave experiments with reflecting coastal structures. Proc. 17th Conf. on Coastal Eng., ASCE, New York, pp. 204–220]. © 1998 Elsevier Science B.V.

*Keywords:* Directional wave analysis; Wave reflection; Field measurements; Coastal structures

---

---

\* Corresponding author.

## **1. Introduction**

The literature concerning the accurate estimation of the directional wave spectra is somewhat vast. However, those articles dealing with methods which remain effective in the presence of phase-locked reflected waves form only a small subset of this literature (e.g., Isobe and Kondo, 1984; Hashimoto and Kobune, 1987). Some articles (e.g., Elgar et al., 1994) have demonstrated the effective field evaluation of the incident and reflective wave field in the presence of reflections. These measurements were obtained at an offshore distance from the reflector which was large enough for the effect of phase coupling to be smoothed over by the spectral analysis technique and therefore have no significant impact on the results. The detection of directional spectra close to structures is of particular importance to the coastal engineer in order to assess accurately the reflection performance of the structure in random directionally spread incident wave fields. Full-scale measurements of wave reflection from coastal structures have normally been confined to 2-dimensional methods of decomposing the incident wave fields, neglecting the effect of oblique wave incidence and directional spread (e.g., Thornton and Calhoun, 1972; Goda and Suzuki, 1976; Davidson et al., 1996). Indeed very little is known about the effect of the angle of wave approach and directional spreading on wave reflection.

Isobe and Kondo (1984) presented a modified form of the maximum likelihood method for the evaluation of the directional wave spectrum in the presence of phase locked reflections. However, the application of this method to field data is in practice somewhat awkward due to the necessary input of the distance from the measurement array to the effective reflection point. Teisson and Benoit (1994) applied the Modified Maximum Likelihood Method (MMLM) and Modified Bayesian method (Hashimoto and Kobune, 1987) of directional analysis to laboratory data and concluded that more work was required in order to assess the precise effective reflection line position. Furthermore, they suggested that the reflection line distance could potentially be added as an additional free parameter in the analysis. In practice the normal assumption that the point of reflection is at the shoreline can lead to large errors in the directional spectra, particularly if the effects of wave shoaling shoreward of the array are ignored.

Additionally, the MMLM is only valid in close proximity to the structure. Further offshore nodes in the standing wave structure close to the sensor locations produce spurious peaks in the directional spectrum. Although the location of these anomalies are predictable, they become ultimately too dense to be effectively removed at a certain offshore distance. At this point one must switch to a more conventional non-phased locked technique (e.g., Maximum Likelihood Method, MLM). The ranges of validity of these techniques are discussed at length in Huntley and Davidson (1997).

The objective of this contribution is to develop a refinement of Isobe and Kondo's method which can be reliably applied to field data without any prior knowledge of the reflection line position.

Firstly, the method of evaluating the 'effective reflection line' position is detailed. The method is then tested with a number of numerical tests. Finally, the technique is applied to field data collected at two reflective field sites, including a rock island breakwater and a vertical sea wall. For field examples where incident waves are

normally incident to the reflector, the frequency dependent reflection function, computed by the new implementation of the MMLM, is compared with a more conventional 2-dimensional technique (Gaillard et al., 1980).

## 2. A method for the practical application of the modified maximum likelihood method

In the absence of phase-locked reflections, the directional wave spectrum  $\hat{S}(\mathbf{k}, \theta)$  may be estimated using the maximum likelihood method (MLM);

$$\hat{S}(\mathbf{k}, \theta) = \kappa \left\{ \sum_m \sum_n \Phi_{mn}^{-1}(\sigma) \exp(i\mathbf{k}[\mathbf{x}_n - \mathbf{x}_m]) \right\}^{-1} \quad (1)$$

Here  $\Phi_{mn}^{-1}$  is the measured inverse cross-spectral density matrix,  $\mathbf{k}$  is the wavenumber vector and  $[\mathbf{x}_n, \mathbf{x}_m]$  are the position vectors of elements  $n$  and  $m$  in a multi-element array (Fig. 1). The symbol  $\kappa$  (Eq. (2)) is a constant of proportionality determined via a comparison of the spectral estimates for each array element and the corresponding estimate of this value obtained from the directional spectrum. Isobe and Kondo (1984) presented a modification to maximum likelihood method which enabled an evaluation of the directional wave spectrum close to a reflector;

$$\hat{S}(\mathbf{k}, \theta) = \kappa \left\{ \frac{\sum_m \sum_n \Phi_{mn}^{-1}(\sigma) \exp(i\mathbf{k}[\mathbf{x}_n - \mathbf{x}_m])}{4 \sum_m \sum_n \Phi_{mn}^{-1}(\sigma) \exp(i\mathbf{k}[\mathbf{x}_{nr} - \mathbf{x}_{mr}])} \left( \sum_m \sum_n \Phi_{mn}^{-1}(\sigma) [\exp(i\mathbf{k}[\mathbf{x}_n - \mathbf{x}_{mr}]) + \exp(i\mathbf{k}[\mathbf{x}_{nr} - \mathbf{x}_m])] \right)^2 \right\}^{-1} \quad (2)$$

Here  $\mathbf{x}_{nr}$ ,  $\mathbf{x}_{mr}$  are the position vectors to elements  $nr$  and  $mr$  in an image of the real array in the reflection line. Notice that the differences between position vectors of elements in the array and image-array are a function of the distance to the effective reflection line. When the seabed is horizontal and the reflector is vertical, the reflection line position is simply the shoreline. In practice however, the seabed is normally sloping or irregular in form. In these circumstances, the distance of the array to the effective reflection line is very difficult to estimate, particularly as reflection does not necessarily occur at the shoreline. Furthermore, estimates of wave celerity calculated using linear wave theory predict that for dispersive waves propagating over a sloping or irregular seabed the reflection line distance (denoted here by rld) is frequency dependent. A constant reflection line position for all frequencies is therefore inappropriate.

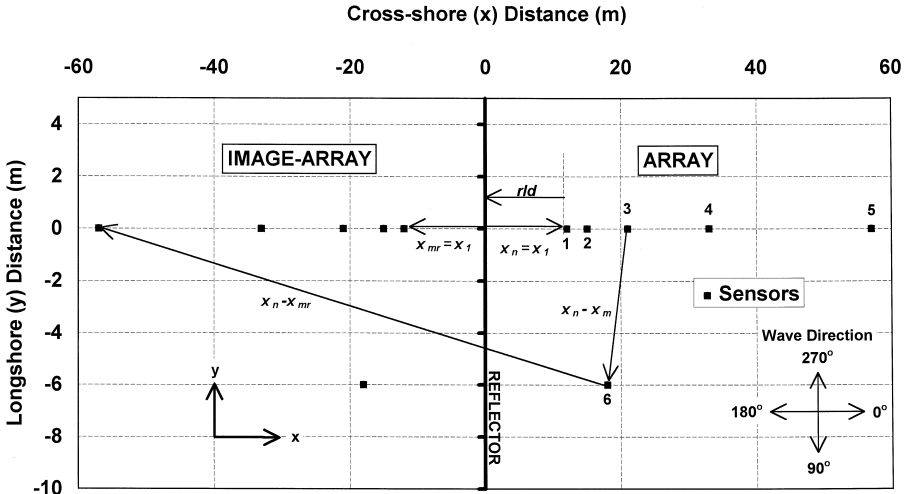


Fig. 1. Definition diagram showing the test array and conventions used in the directional analysis.

The second term on the right hand side of Eq. (2), which is subtracted from the MLM estimate, is set to zero when the reflection coefficient defined by;

$$\frac{\sum_m \sum_n \Phi_{mn}^{-1}(\sigma) [\exp(ik[x_n - x_{mr}]) + \exp(ik[x_{nr} - x_m])] }{2 \sum_m \sum_n \Phi_{mn}^{-1}(\sigma) \exp(ik[x_{nr} - x_{mr}])} \tag{3}$$

is less than or equal to zero and the MMLM (Eq. (2)) reduces to the MLM (Eq. (1)). The constant of proportionality  $\kappa$  in Eqs. (1) and (2) is given by:

$$\kappa_{mm}(\sigma) = \frac{\Phi_{mm}(\sigma)}{\int_{k_i} [\hat{S}(k_i, \sigma) + 2\sqrt{\hat{S}(k_i, \sigma)\hat{S}(k_r, \sigma)} \cos k_i(x_m - x_{mr}) + \hat{S}(k_r, \sigma)] dk_i} \tag{4}$$

Where the subscripts  $i$  and  $r$  represent the incident and reflected wave components respectively. Notice that  $\kappa_{mm}$  can be evaluated for each frequency and each element  $m$  of the array. Normally the mean value ( $\bar{\kappa} = \frac{1}{m} \sum_m \kappa_{mm}$ ) is evaluated for use in Eq. (2). Alternatively, a linear least squares regression between the numerator and denominator of Eq. (4) for each array element will provide an overall estimate of  $\kappa$ . This latter analysis also presents a further possibility. The correlation coefficient  $r$  of the least squares regression is an indication of how faithfully the predicted estimate of variance

from the MMLM matches the observed value for each array element. It is assumed here (and established later) that this correlation coefficient is a function of the error in the reflection line estimate. Thus, using an iterative process to minimise an error function of the form;

$$\varepsilon = \frac{(1 - r)}{2} \quad (5)$$

can provide a means of estimating an unknown reflection line distance. Here the error function (Eq. (5)) will be zero if there is a perfect linear correlation between the numerator and denominator of Eq. (4), one if there is a perfect inverse correlation and, a half for zero correlation.

Eq. (5) is minimised for each frequency bin, thus allowing for any frequency dependence in the reflection line position. The method of minimisation used here is based on a golden section search and parabolic interpolation method (Forsythe et al., 1976). This routine requires an input of the interval (range in rld values) within which the minimum value of Eq. (5) is to be found. The domain of the search is a user input to the programme. Typically an interval for the search is selected, which is centered on the theoretical reflection line position assuming that reflection takes place at the shoreline (see Eq. (11) discussed later). The width of the rld domain searched typically increases with offshore distance as the uncertainty in the rld position increases. For example if the expected reflection line position is around 12 m from the array, a typical rld interval might be  $0 \text{ m} < \text{rld} < 25 \text{ m}$ , whereas if the expected reflection line position is 50 m the search domain might be  $25 \text{ m} < x < 75 \text{ m}$  approximately doubling the search interval. Extending the domain of the search increases the computational time required to minimise Eq. (5) to within the required tolerances. Here the rld value has been estimated to the nearest millimetre. Outliers in the rld estimate are sometimes produced if the total rld interval is greater than or equal to one wavelength. This occurs as the error function exhibits some periodicity with the rld, the length scale of which corresponds to the incident wavelength at that frequency. Thus, at high frequencies it is sometimes necessary to reduce the range in rld values searched to a value close to, but less than the incident wavelength ( $\lambda$ ) at that frequency (e.g.,  $0.9 \lambda$ ). If the minimisation yields rld values which are close to the extremes of the chosen interval, this indicates that an inappropriate choice has been made and the analysis should be repeated selecting a broader rld interval.

This method assumes that at a given frequency wave components from all directions are reflected from the same cross-shore position and that reflection occurs principally along one line and is not a distributed process. If the reflection process was distributed across the nearshore profile then it is likely that the cross-shore node/antinode structure would be significantly reduced and a standard directional analysis method (e.g., MLM) may be appropriate.

The effectiveness of this method for detecting an unknown reflection line will be a function of the array geometry, the presence of signal noise, the incident wave characteristics and the distance from the reflector. For an assessment of the method, we turn to a numerical simulation.

### 3. Numerical tests

#### 3.1. Method of simulation

Simulated time-series for a spatially separated, 6-element array were computed using the following methodology:

1. The directional energy distribution of the incoming wave field was estimated using a Mitsuyasu et al. (1975) directional distribution of the form;

$$S(\theta) = \cos^{2s}\left\{(\theta - \theta_p)/2\right\} \quad (6)$$

where  $\theta_p$  is the principal wave direction and  $s$  is the directional spreading parameter.

2. The frequency distribution of the wave spectrum was estimated using the ISSC spectrum of the form:

$$S(f) = \frac{0.313 H_s^2 f_m^4}{f^5} \exp\left(\frac{-1.25 f_m^4}{f^4}\right) \quad (7)$$

Here  $H_s$  is the significant wave height and  $f_m$  is the spectral peak frequency.

3. Time-series 4096 data points long are simulated using Gaussian white noise so as to generate a white spectrum of wave frequencies (Huntley et al., 1996). One time series is generated for each directional component computed using Eq. (6). 181 directional components are generated at 1-deg increments  $90^\circ$  either side of (and including) the principal wave direction ( $\theta_p$ ).

4. Each of the time-series are Fast Fourier Transformed into the frequency domain and shaped according to frequency and directional energy distributions given by Eq. (7) and Eq. 8.

5. Phase-locked reflected time series were computed by applying a phase lag ( $L$ ) to the incident series given by;

$$L = \frac{2r \text{ld} \cos(\theta_p)}{c} \quad (9)$$

where  $c$  is the phase velocity. In these simulations the long wave approximations have been made therefore  $L$  has a constant value for all frequencies.

6. All series are reverse transformed into the time domain. Each of the angular components are summed to give a single time-series.

7. 1–6 above are repeated for each element of the array adding an appropriate lag in the frequency domain which reflects the spatial offset of the wave gauges.

8. Finally, incident and reflected time-series for each array element are summed after weighting the reflected series with a user defined reflection coefficient ( $K_r(f)$ ).

Having generated the synthetic time series, directional spectra were computed using Eqs. (1)–(5). Spectral estimates were computed using a full Hanning window of 512 data points in length with 50% overlapping segments, giving spectral estimates with 27 degrees of freedom (Nutall, 1971). The sampling frequency was 4 Hz and the geometry of the 6-component test array is shown in Fig. 1.

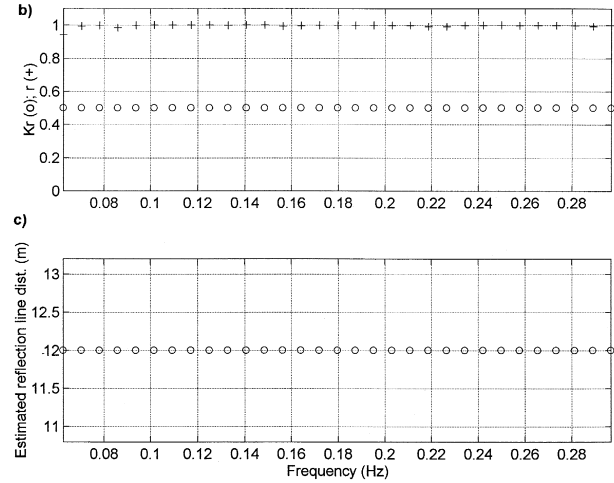
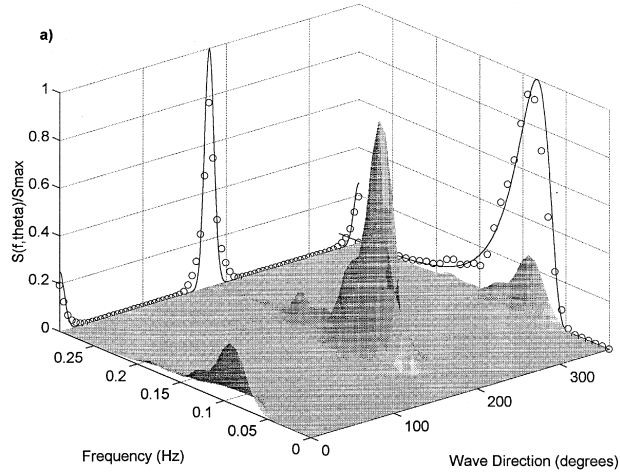


Fig. 2. (a) Diagram showing the directional wave spectrum computed using the MMLM on simulated data with no reflection line distance specified. Target (solid lines ‘—’) and estimated values (open circles ‘○’) of  $S(f)$  and  $S(\theta)$  are shown projected on the side walls of this plot. [ $T = 12$  s,  $rld = 12$  m,  $s = 200$ ,  $\theta_p = 180^\circ$ ,  $L/S = 0.025$ , added noise = 0%,  $K_r(f) = 0.5$ ]. (b) Plot of the correlation coefficient ( $r$ ) between measured and estimated surface elevation variance (crosses ‘+’) and reflection coefficient  $K_r$  (open circles ‘○’) as a function of frequency. (c) Reflection line distance evaluated by minimising Eq. (5). In (b) and (c) values are plotted only for the energetic region of the spectrum (defined here as  $> 0.01 S_{max}$ ).

### 3.2. Simulation results

In this section the directional analysis technique outlined in Section 2 is applied to various synthetic data sets. Simulations are run with; a) different spectral peak frequencies, wave directions and directional spread; b) added noise; c) different reflection line positions, and d) a reduced array of only four transducers. In each case an assessment is made of the accuracy to which the simulations are reproduced by the directional estimates, the validity of the frequency dependent reflection coefficient estimate and the predicted versus the specified reflection line position. For all of the directional spectra presented here the reflection line position is unspecified in the directional analysis.

Fig. 2a shows the MMLM directional wave spectrum computed for  $T = 12$  s,  $s = 200$ , a water depth of  $d = 6$  m and a reflection line distance of  $rld = 12$  m. Here the reflection line has been specified in the simulation but not in the directional analysis. Projected on the side walls of the 3-dimensional plots in the open circles are the frequency and directionally integrated spectra ( $S(\theta)$  and  $S(f)$ ) computed from  $S(f, \theta)$ . Here the target spectra are also shown by the solid lines for comparison with the estimates. Notice that for ease of comparison, the directional and target spectra have been normalised by their maximum. Estimates of  $S(f)$  and  $S(\theta)$  have also been normalised by the same value as their corresponding target spectra. In this example, waves are normally incident with a peak direction at  $180^\circ$  and reflected waves occur at  $0^\circ$ . The directional and frequency resolutions are  $5^\circ$  and 0.0078 Hz respectively. In all cases the reflection coefficient ( $K_r(f)$ ) is set at 0.5.

Fig. 2b shows that there is an excellent comparison between the estimated and target spectra. In fact, the estimated directional spectrum is not improved further by actually specifying the known reflection line position in the directional analysis. The directional distribution is particularly good. There is some deviation between the target and estimated values of  $S(f)$  which is likely to be a function of the uncertainty associated with the spectral estimate.

Fig. 2b and c show the correlation coefficient  $r$  (crosses, Fig. 2b), frequency dependent reflection coefficient  $K_r(f)$  (open circles, Fig. 2b) and estimated reflection line position (Fig. 2c), all as a function of frequency. Here the values are presented for data with energy levels above  $0.01 S_{\max}$ , where  $S_{\max}$  is the spectral peak value of the averaged frequency spectra for all sensors.  $K_r(f)$  has been defined by:

$$K_r(f) = \sqrt{\frac{\int_{\theta_r} S(f, \theta_r) d\theta}{\int_{\theta_i} S(f, \theta_i) d\theta}} \quad (10)$$

where  $\theta_i$  and  $\theta_r$  represent the incident and reflected wave directions respectively. In all cases the correlation coefficient is near unity, errors in  $K_r(f)$  are less than 0.1% and the reflection line distance is accurate to within a fraction of a centimetre of its defined value of 12 m relative to sensor No. 1.

Fig. 3 shows the distribution of the error function (Eq. (5)) that was minimised in order to obtain the estimates in Fig. 2 with both frequency and offshore distance. Notice

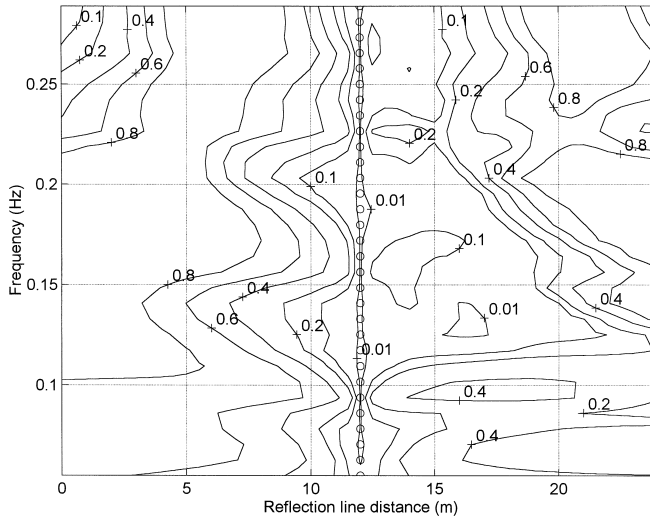


Fig. 3. Plot of the error parameter for Fig. 2 (Eq. (5)) as a function of reflection line distance and frequency. Notice that the actual value of  $rld = 12$  m is shown by the minima on this plot. Also notice the estimated reflection line position (open circles 'O') obtained by minimising Eq. (5).

the minima associated with true  $rld$  value at 12 m. The open circles at  $x = 12$  m on this figure are the results of a minimisation routine used to locate the reflection line position.

Fig. 4a,b and c shows an equivalent analysis to Fig. 2 above but with a much broader directional spread ( $s = 20$ ). Again the directional spectra and  $K_r(f)$  have been faithfully reproduced by the directional analysis. Although the estimate of the reflection line position shows a slightly larger deviation from the defined value, errors are still less than 20 cm.

Fig. 5a,b and c show the combined effects of reducing the spectral peak period to 8 s, and oblique wave incidence at  $40^\circ$  to the normal (peak direction  $140^\circ$ ). Estimates of the reflection line position degrades both with oblique wave incidence and towards higher frequencies ( $> 0.3$  Hz). These factors relate to the resolution capabilities of the test array which are a function of frequency and wave direction. Maximum errors in the estimated reflection line position are 70 cm which give rise to errors in the frequency dependent reflection coefficient of up to 15%. However, the *frequency averaged* reflection coefficient shows negligible errors ( $< 0.4\%$ ).

Fig. 6 Fig. 7 show the effects of adding noise to the simulated time-series. Signal to noise ratios for Figs. 6 and 7 are 10 and 20, respectively. The added noise has the effect of broadening the directional spread of the spectrum beyond that of the target distribution, and increases errors in the estimates of the reflection line position and  $K_r(f)$ . For a signal to noise ratio of 20 the reflection line position is consistently overestimated (by up to 70 cm) and the frequency dependent reflection function shows a bias of up to 21%. The observed bias in  $K_r(f)$  increases towards high frequency in the tail of the spectrum where signal to noise ratios are worse than the more energetic region of the spectrum.

Next we investigate the effect of the reflection line position. Huntley and Davidson

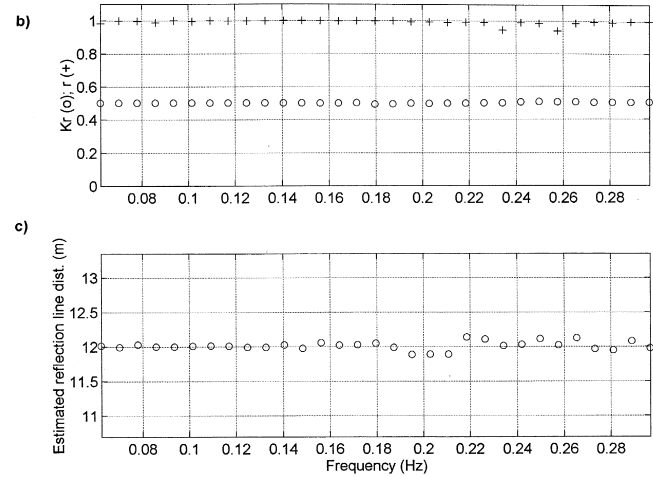
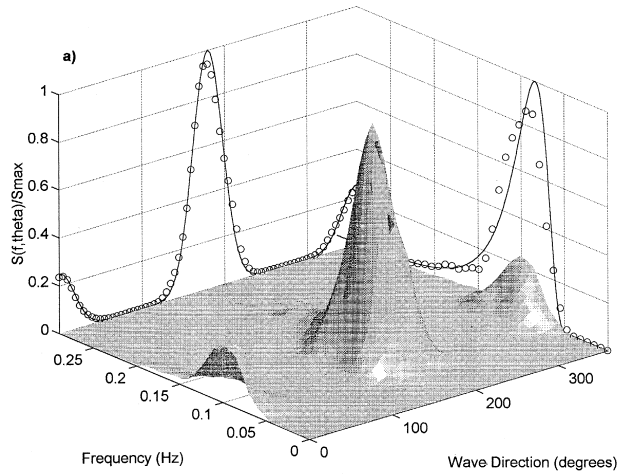


Fig. 4. (a,b and c) These figures show a similar directional analysis to that illustrated in Fig. 2 but with a much broader directional spread in the incident waves. [ $T = 12$  s,  $r_{ld} = 12$  m,  $s = 20$ ,  $\theta_p = 180^\circ$ ,  $L/S = 0.025$ , signal/noise = 0,  $K_r(f) = 0.5$ ].

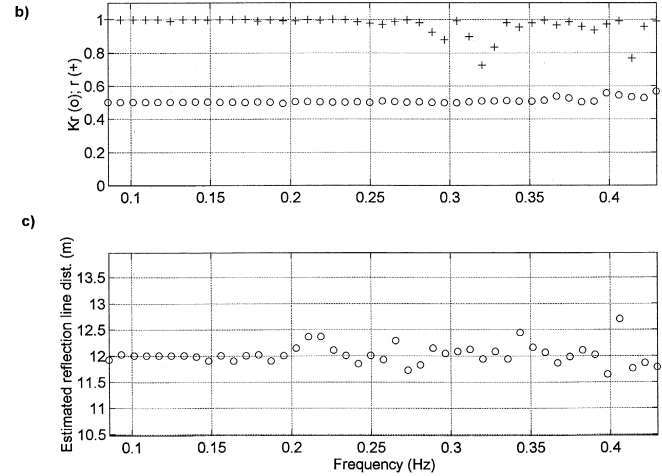
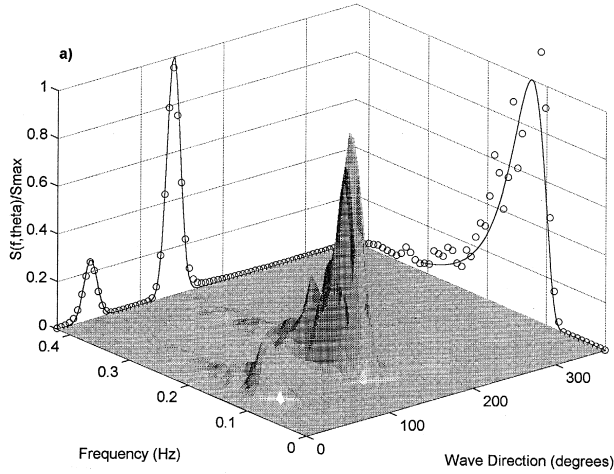


Fig. 5. (a,b and c) These figures show a similar directional analysis to that illustrated in Fig. 2 but for oblique wave incidence and higher frequency incident waves. [ $T = 8$  s,  $rld = 12$  m,  $s = 100$ ,  $\theta_p = 140^\circ$ ,  $L/S = 0.025$ , signal/noise = 0,  $K_r(f) = 0.5$ ].

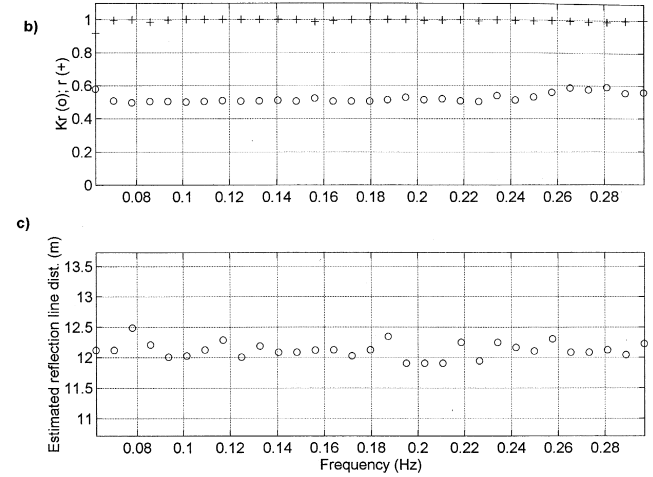
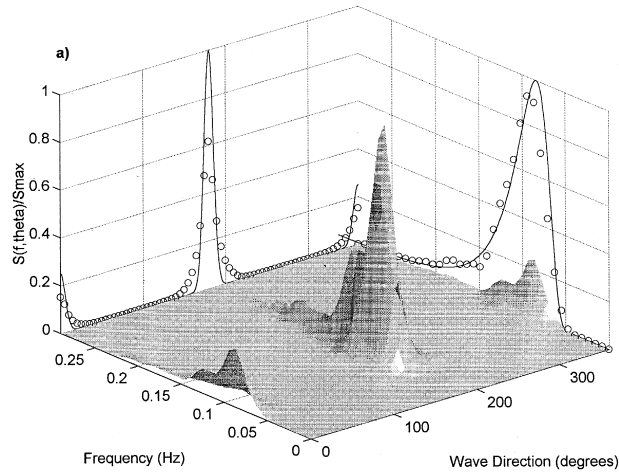


Fig. 6. (a,b and c) These figures show a similar directional analysis to that illustrated in Fig. 2 but with a signal to noise ratio of 10. [ $T = 12$  s,  $r_{ld} = 12$  m,  $s = 200$ ,  $\theta_p = 180^\circ$ ,  $L/S = 0.025$ , **signal/noise = 10**,  $K_r(f) = 0.5$ ].

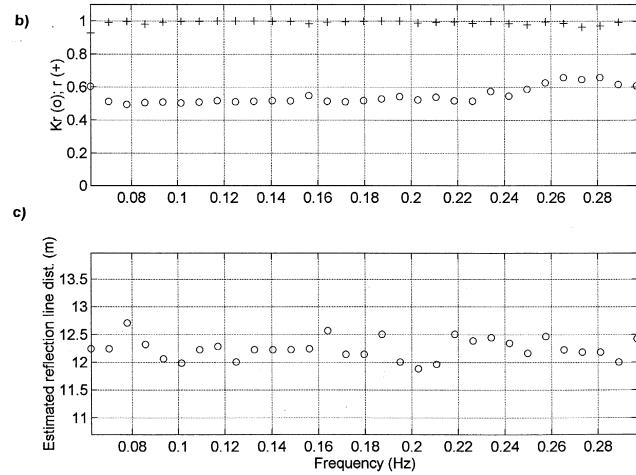
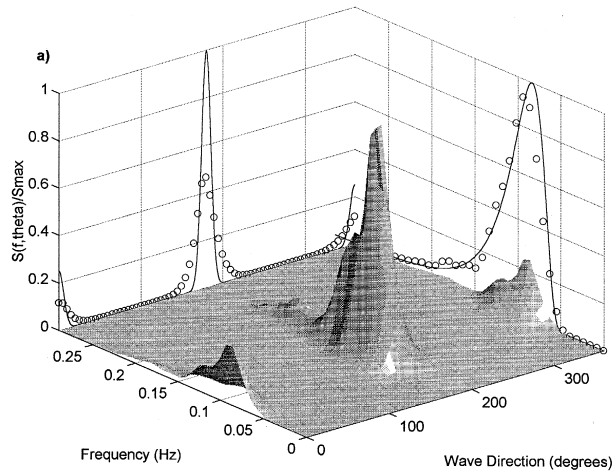


Fig. 7. (a, b and c) These figures show a similar directional analysis to that illustrated in Fig. 2 but with a signal to noise ratio of 20. [ $T = 12$  s,  $rld = 12$  m,  $s = 200$ ,  $\theta_p = 180^\circ$ ,  $L/S = 0.025$ , **signal/noise = 20**,  $K_r(f) = 0.5$ ].

(1997) explored the relative domains of phase locked (MMLM) and non-phase locked (MLM) directional analysis methods in terms of the dimensionless parameter  $L/S$ , where  $L$  is normal lag given by Eq. (9) with  $\theta$  set to zero, and  $S$  is the segment length of the Fourier transform. In these simulations,  $L$  represents the non-dispersive phase lag. Thus, the ratio  $L/S$  has a constant value for all frequencies. It should be noted however, that in intermediate and deep water  $L/S$  will be frequency dependent.

For large values of  $L/S$  ( $> 0.5$ ) the phase coupling is smoothed over by the spectral analysis technique, and non-phase locked techniques can accurately evaluate the directional wave spectrum. In this regime, ( $L/S > 0.5$ ) phase locked techniques are unnecessary and inappropriate due to large amplification of signal noise at regions in  $\hat{S}(\mathbf{k}, \theta)$  where nodes are predicted close to the sensor locations.

At lower values of  $L/S$  ( $< 0.025$ ) non-phase locked methods do not provide an accurate measure of the directional wave spectrum and phase-locked methods (requiring an estimate of the reflection line position) can be used to provide accurate estimates of the directional spectrum free from spurious peaks.

Between these two regimes ( $0.025 < L/S < 0.5$ ), neither phase locked or non-phase locked techniques are ideally suited. Huntley and Davidson used numerical simulations to show that non-phase locked methods could be extended down to  $L/S$  ratios as low as 0.2 providing some loss (a factor of 2) in the directional resolution could be tolerated. Additionally, multi-element arrays like the six gauge array used here could be used to stretch the regime of phase locked methods, the effect of a node at one sensor location effectively being nullified by data from other sensors. It was found that a six gauge array could provide reasonable directional spectra using the MMLM for  $L/S$  ratios up to and sometimes exceeding  $L/S = 0.13$  providing the array was designed carefully. Thus, the problem zone where neither the MLM or the MMLM can be used to estimate the directional spectrum corresponds to  $0.13 < L/S < 0.2$ .

Fig. 8a,b and c Fig. 9a,b and c show the results of the directional analysis of similar synthetic time-series to that analysed in Fig. 2a (rld = 12 m,  $L/S = 0.025$ ) but for reflection line distances of 64 m ( $L/S = 0.13$ ) and 246 m ( $L/S = 0.5$ ) respectively. At  $L/S = 0.13$  (Fig. 8) the directional spectrum is still well reproduced by the MMLM although the directional resolution has degraded slightly due to errors of up to 90 cm in the estimated reflection line position. Errors in  $K_r(f)$  however, are still less than 5% for  $L/S = 0.13$ . Further offshore of the reflector at  $L/S = 0.5$ , erroneous ridges begin to develop in the directional spectrum (Fig. 9a), the reflection line estimate is in error by up to 16 m and the frequency dependent reflection coefficient shows a maximum bias of 38%.  $L/S = 0.5$  is the domain of non-phase locked method and perfect results (not shown here) can be obtained by implementing the MLM which requires no knowledge of the reflection line position.

The final test presented here is with a reduced number of sensors. Fig. 10a,b and c show an equivalent analysis to Fig. 2 but with only four transducers. Here transducers 3 and 6 (see Fig. 1) have been omitted from the simulation array. Inspection of Fig. 10 shows that the directional resolution has been quite badly degraded but reflection coefficient estimates remain very accurate. It should be noted that a better array design with one of the transducers offset in the  $y$ -direction would significantly improve the directional resolution.

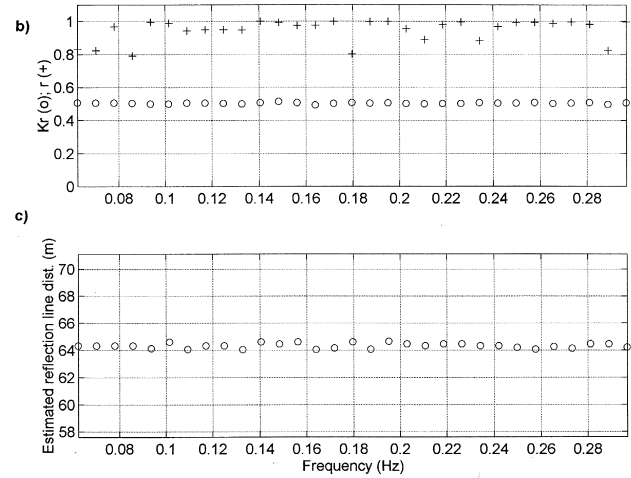
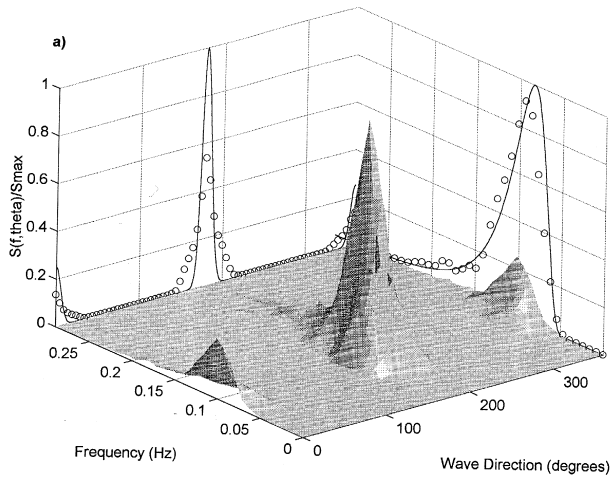


Fig. 8. (a,b and c) These figures show a similar directional analysis to that illustrated in Fig. 2 but with an extended reflection line distance (and  $L/S$  ratio). [ $T = 12$  s,  $rd = 64$  m,  $s = 200$ ,  $\theta_p = 180^\circ$ ,  $L/S = 0.13$ , signal/noise = 0,  $K_r(f) = 0.5$ ].

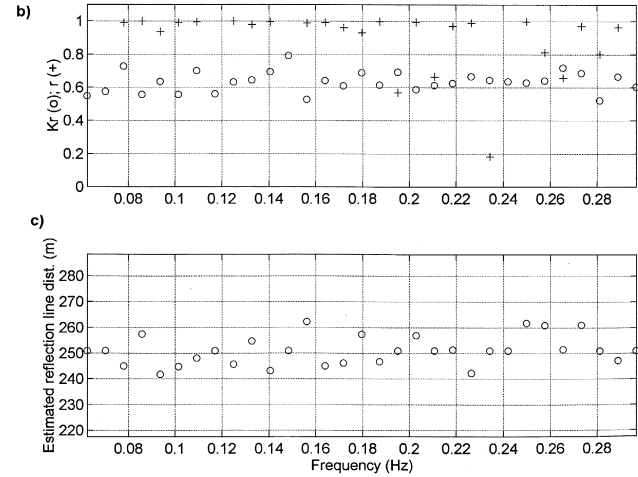
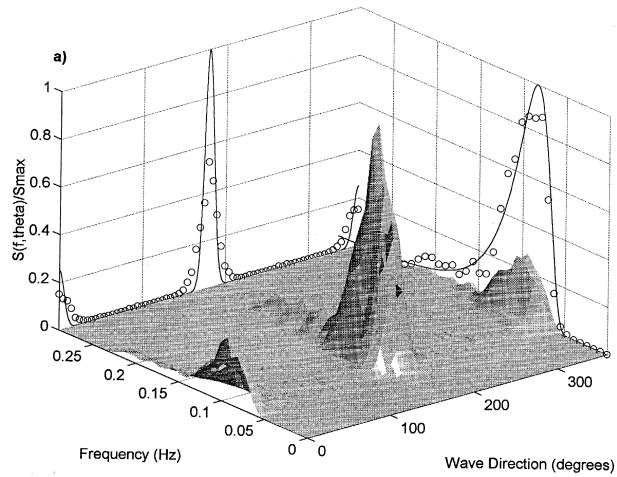


Fig. 9. (a,b and c) These figures show a similar directional analysis to that illustrated in Fig. 2 but with an extended reflection line distance (and  $L/S$  ratio). [ $T = 12$  s,  $rld = 246$  m,  $s = 200$ ,  $\theta_p = 180^\circ$ ,  $L/S = 0.5$ , signal/noise = 0,  $K_r(f) = 0.5$ ].

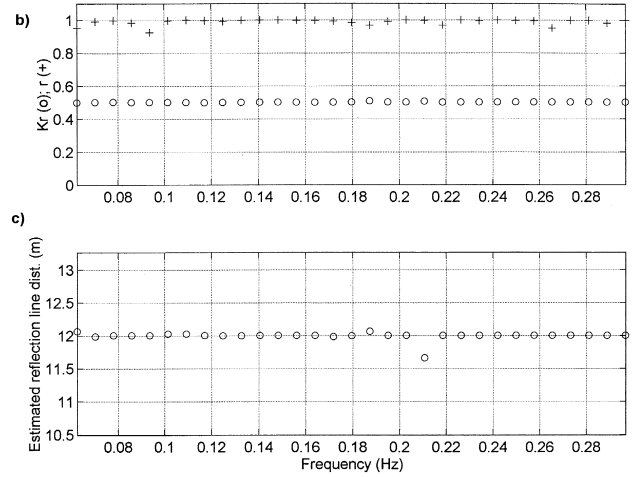
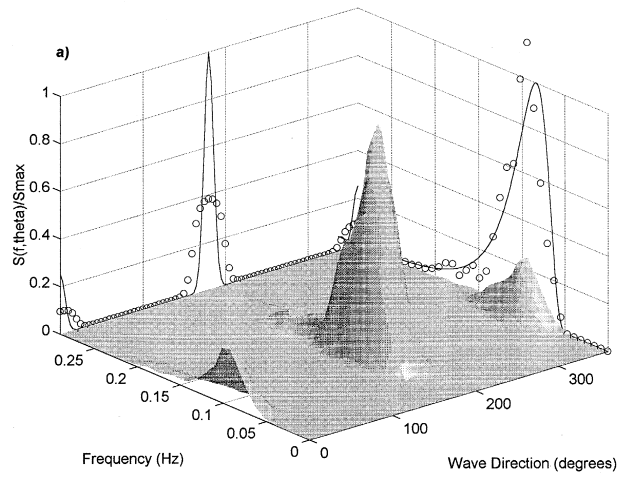
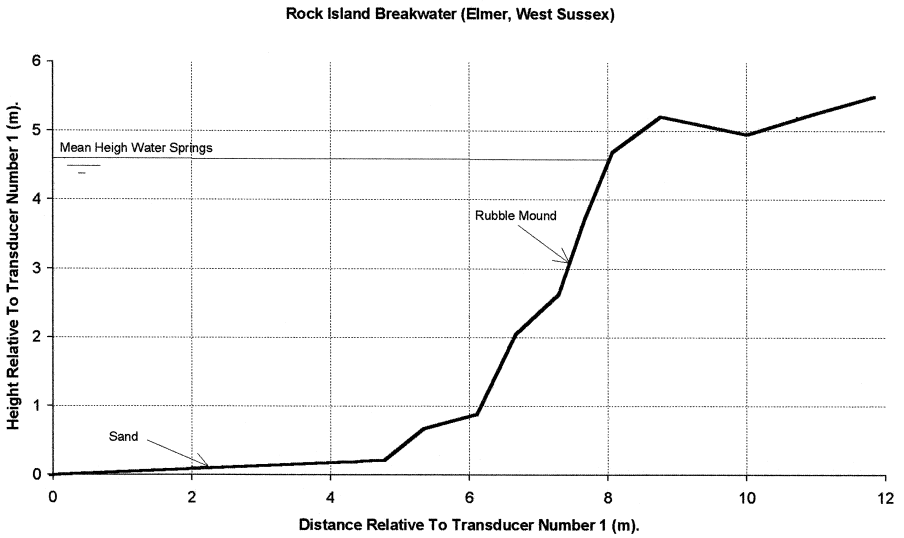


Fig. 10. (a,b and c) These figures show a similar directional analysis to that illustrated in Fig. 2 but with only 4 sensors. Transducers 3 and 6 in Fig. 1 have been omitted from the analysis. [ $T = 12$  s,  $r_{ld} = 12$  m,  $s = 200$ ,  $\theta_p = 180^\circ$ ,  $L/S = 0.025$ , signal/noise = 0,  $K_r(f) = 0.5$ , 4 sensors].

### 4. Analysis of field data

In this section the directional analysis method outlined in Section 1 is applied to field data from two sites. The first is a rock island breakwater in Elmer, West Sussex

a)



b)

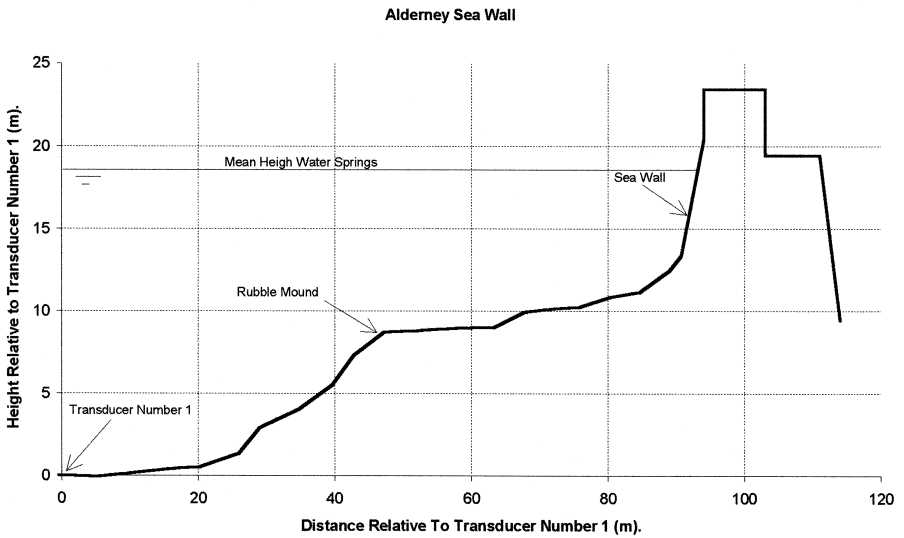


Fig. 11. Cross-shore profiles for: (a) A rock island breakwater at Elmer, West Sussex, UK and (b) Alderney Breakwater, Channel Islands, UK.

(Davidson et al., 1994, 1996), and the second is an impermeable sea wall at Bray Harbour, Alderney in the Channel Islands. The cross-shore profiles of the two structures are shown in Fig. 11a and b. In both cases, a pressure transducer array (Bird et al., 1994) of similar design to that used in the numerical tests was deployed seawards of the structures. Heights and distances in Fig. 11 are given relative to the most shorewards sensor in the array. Average  $L/S$  ratios for Elmer and Alderney sites are 0.025 and 0.2 respectively.

Fig. 12a shows MLM (non-phase locked) directional spectrum for steep ( $H_{mo}/\lambda_p = 0.031$ )<sup>1</sup> sea waves at the rock island breakwater site. The directional spectrum estimate shows an unrealistically large directional spread. The low  $L/S$  ratio of 0.02 for this data indicates that the data falls clearly in the domain of the phase locked directional analysis methods and the MLM is inappropriate. Fig. 12b shows the MMLM analysis of the same data set (with no reflection line distance specified) yielding clearly defined incident waves at  $180^\circ$  (normal to the structure), and reflected waves at  $0^\circ$  with much reduced directional spread compared to the MLM results.

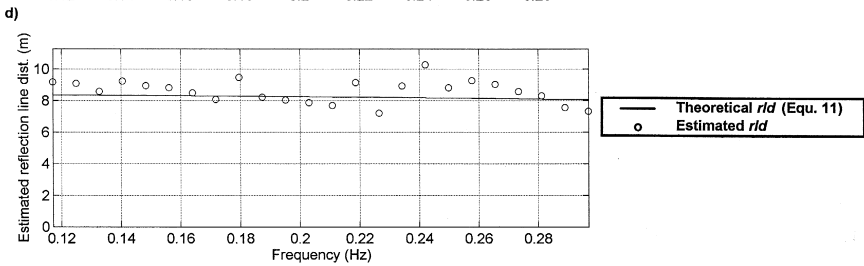
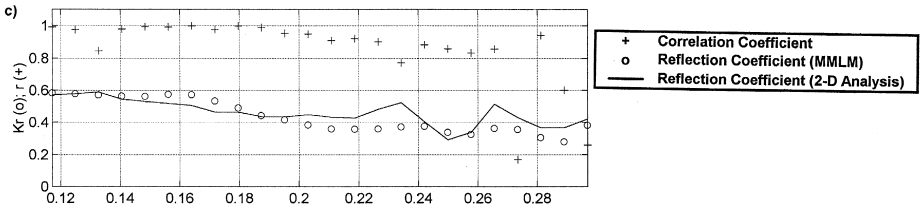
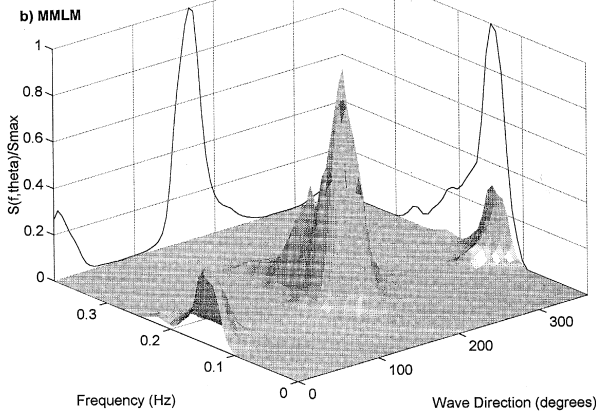
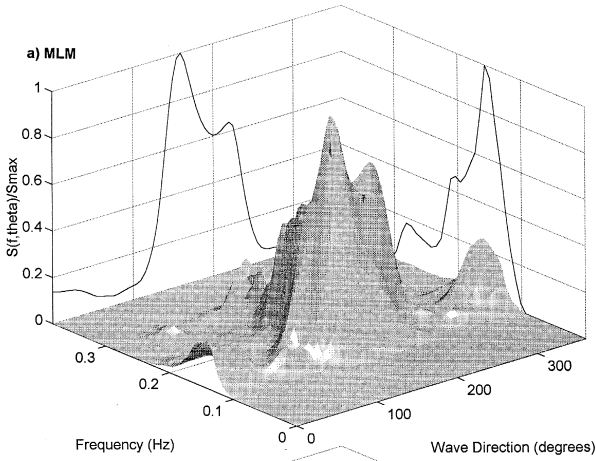
Fig. 12c shows the corresponding correlation coefficient (crosses) and frequency dependent reflection function (open circles) for Fig. 12b. Data shown here are for the frequency band for which energy levels exceed  $0.05 S_{max}$ . Correlation coefficients are generally high particularly in the energetic region of the spectrum and frequency dependent reflection coefficient decreases gradually with increasing frequency. Since the waves are normally incident to the breakwater, this provides an excellent opportunity for a comparison with a two dimensional reflection analysis. The solid line in Fig. 12c represents the frequency dependent reflection coefficient evaluated using the 2-D method of Gaillard et al. (1980). Encouragingly, there is an excellent agreement between the 2-D and 3-D (MMLM) estimates of  $K_r(f)$ . This is consistent with the findings of Teisson and Benoit (1994) who found good agreement in  $K_r(f)$  between both the MMLM, Modified Bayesian Method and the 2-D least squares solution of Mansard and Funke (1980) when applied to laboratory data.

Fig. 12d illustrates the estimated position of the reflection line (open circles) relative to the most shorewards transducer. Also shown is the theoretical reflection line distance obtained by numerically integrating the phase velocity given by linear wave theory over the profile between the most shorewards transducer and the still water level, where;

$$\text{rld}(k) = \frac{x_1 \tanh(kd_1)}{\int_{x=0}^{x=x_1} \tanh(kd(x)) dx} \quad (11)$$

Here  $x_1$  and  $d_1$  are the offshore distance and depth at transducer number 1,  $k$  is the wave number, and  $d(x)$  is the local water depth taken from the survey (Fig. 11). Notice that the nearshore profile between the array and the shoreline must be known in order to evaluate Eq. (11). Fig. 12d shows an excellent agreement between the theoretical and

<sup>1</sup>  $H_{mo}$  is equal to 4 times the standard deviation of the wave record and  $\lambda_p$  is the spectral peak wavelength.



observed reflection line position for a  $d_1$  value of 3.6 m. The theoretical reflection line position given by Eq. (11) is always landwards of the still water level due to waves shoaling and slowing down in the shallower water shoreward of the sensors. No allowance is made here for wave setup ( $\bar{\eta}$ ) although calculations show that the setup correction would be relatively small ( $\bar{\eta} < 12$  cm) in the low amplitude wave conditions analysed here.

Good estimates of directional spectra may be obtained for the rock island breakwater site by computing the reflection line distance directly from Eq. (11) and using the standard MMLM technique. It is computationally most efficient to implement Eq. (11) in the form of a 'lookup table' which is entered with known values of depth and frequency. However, it cannot always be assumed that reflection takes place at the shoreline. If reflection takes place offshore of the shoreline (e.g., over a sand bar), inaccurate results would be obtained from Eq. (11) and modified MMLM presented here would be more appropriate. Additionally, Guza and Bowen (1976) found that a significant phase change occurred in waves reflected from a smooth laboratory beach with a slope of  $7^\circ$  if the reflection coefficient was less than 0.4. Such a phase change would also cause errors in the predicted reflection line position using Eq. (11).

A similar analysis is shown for low steepness ( $H_{mo}/\lambda_p = 0.004$ ) swell waves in Fig. 13a, b and c. Again the directional spectrum appears to be well resolved, there is excellent agreement between the frequency dependent reflection function evaluated with the 2-D and 3-D methods and the estimated reflection line position is close to the theoretical value. Notice that the reflection coefficient is higher than in Fig. 12c due to the low steepness of the waves. Also notice that the estimated reflection line position has moved slightly shoreward in Fig. 13c compared to Fig. 12d due to an increase in the tidal level ( $d_1 = 4.38$  m).

Two further examples of directional spectra are shown for the rock island breakwater for broad- and narrow-banded incident wave spectra (Fig. 14a and b respectively) illustrating the versatility of this directional analysis method.

Fig. 15 shows directional spectra computed for the Alderney Harbour sea wall. The upper panel (Fig. 15a) is the result of the MLM which produced a realistic directional spectrum showing strong reflection as expected at this site. Numerical tests carried out by Huntley and Davidson (1997) indicate that the non-phase locked method is expected to perform reasonably well at the  $L/S$  ratio for this data set of 0.2 although some (a factor of 2) degradation in the relative angular half-power spectral width can be expected. The performance of the MLM at this site is perhaps aided by both the directional spread of the incident waves and distributed reflection from the rubble mound fronting the sea wall. Both these processes would lead to a de-coupling of the incident and reflected wave components.

---

Fig. 12. (a) An MLM analysis of field data collected in front of a rock island breakwater (Elmer, West Sussex, UK) at 0912 on 12/06/92 ( $H_{mo} = 1.16$  m,  $L/S = 0.02$  m,  $H_{mo}/\lambda_p = 0.031$ ). (b) Analysis of the same data file as (a) but using the MMLM with no reflection line position specified. (c) Correlation coefficient and reflection coefficients estimated using the MMLM and a 2-dimensional analysis method. (d) Estimated reflection line position and theoretical reflection line position given by Eq. (11).

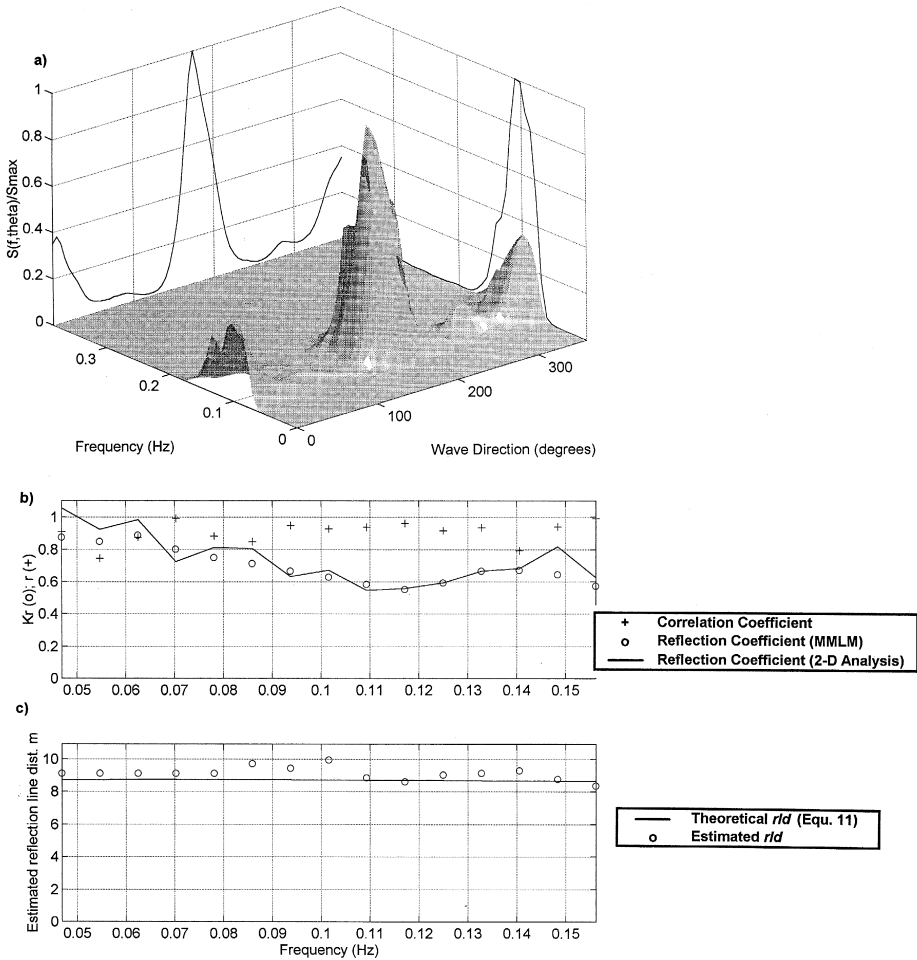


Fig. 13. (a) An MMLM analysis (with no reflection line specified) of very low steepness waves measured in front of a rock island breakwater (Elmer, West Sussex, UK) at 0134 on 5/07/92 ( $H_{mo} = 0.24$  m,  $L/S = 0.02$  m,  $H_{mo}/\lambda_p = 0.004$ ). (b) Correlation coefficient and reflection coefficients estimated using the MMLM and a 2-dimensional analysis method. (c) Estimated reflection line position and theoretical reflection line position given by Eq. (11).

The equivalent analysis using the MMLM method with no reflection line specified (Fig. 15b) shows a poor directional spectrum with large spurious glitches between the incident and reflected peaks. The spurious glitches are larger than those predicted in the numerical simulations for  $L/S = 0.5$  due to the presence of some noise in the real data. Although these glitches are predictable (see Huntley and Davidson, 1997) and are potentially removable better directional estimates can be obtained using the MLM. Clearly, for  $L/S > 0.2$  we must rely on non-phase locked methods.

Fig. 15c shows that in spite of the glitches in the directional spectrum (Fig. 15a) the correlation coefficient (crosses) between the predicted and observed surface elevation

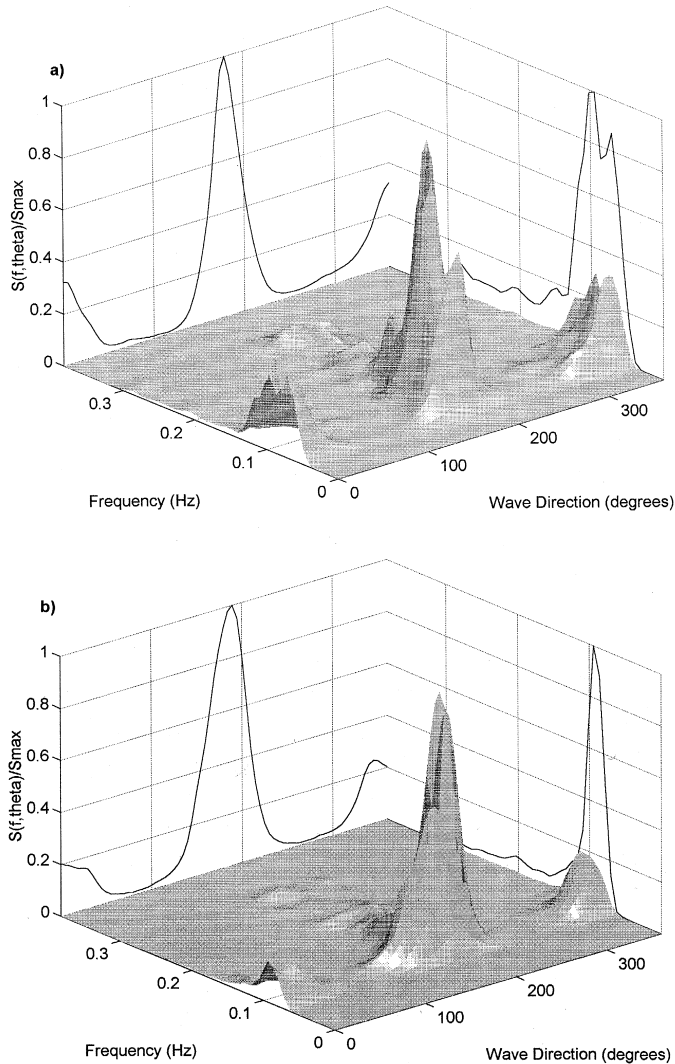
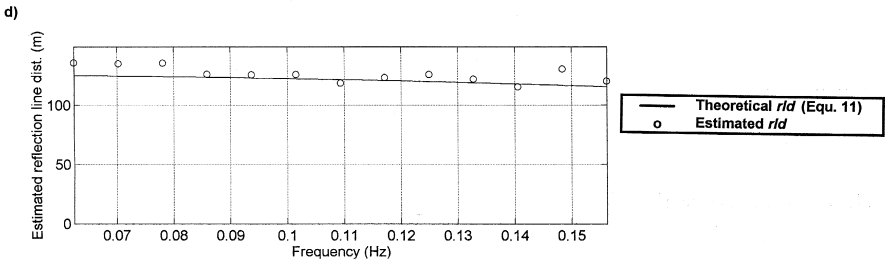
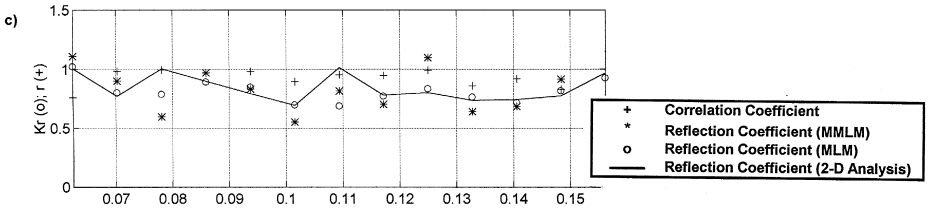
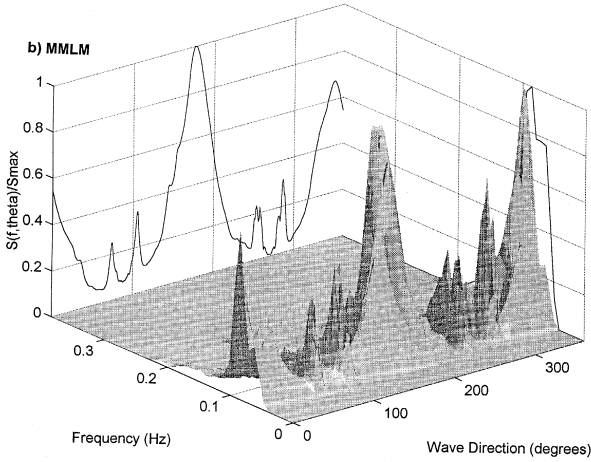
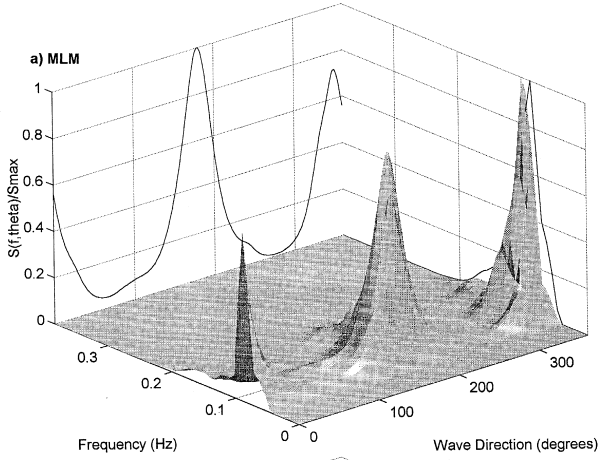


Fig. 14. Directional analysis (MMLM with no reflection line specified) of (a) broad and (b) narrow banded waves collected on the 4/7/92 and the 3/7/92 respectively at Elmer, West Sussex.

variance at the sensor locations is reasonably high ( $> 0.75$ ). The estimated reflection line position (open circles in Fig. 15d) also closely matches the theoretical value given by Eq. (11) (solid line in Fig. 15d).

The frequency dependent reflection function is also shown in Fig. 15c for the MLM (open circles), MMLM (stars) and the 2-D method (solid line). Generally the agreement between the 2-D and MLM estimate of  $K_r(f)$  is good. The 2-D method which utilises only 3-gauges is prone to overestimating the reflection coefficients at frequencies where the coherence between sensors is low due to the close proximity of a sensor to a node



(e.g., at 0.109 Hz). The  $K_r(f)$  estimate computed from the MMLM is unreliable due to the spurious glitches in the spectrum.

## 5. Concluding remarks

A method has been developed for the accurate determination of directional spectra which requires no prior knowledge of the reflection line position in phase locked, reflective sea states. Numerical tests have shown that the technique is robust; in different sea states (with different directional spread, peak periods, angles of incidence), in the presence of signal noise, with only a limited number (4) of sensors, and  $L/S$  ratios up to 0.13.

Field tests have verified the numerical predictions of Huntley and Davidson (1997) which predict the relative domains of phase locked and non-phase locked directional analysis methods as a function of  $L/S$ . Here,  $L$  is the time lag associated with the travel time required for a wave to pass over the sensors and return after reflection, and  $S$  is the duration of the Fast Fourier Transform segment. The new phase locked MMLM method performed well when applied to field data with an  $L/S$  ratio  $\approx 0.025$  and that non-phase locked MLM method (requiring no reflection line information) was found to be appropriate for an  $L/S$  ratio of 0.2. For field tests where incident waves are normal to the structure good agreement was found between the frequency dependent reflection functions analysed using both the 3-D MMLM or MLM and 2-D Gautier et al. (1982) methods.

Field data collected at a rock island breakwater and vertical sea wall showed good agreement between estimated and theoretical (Eq. (11)) reflection line positions indicating that *in these examples* where reflection coefficients are high ( $K_r(f) > 0.4$ ) reflection takes place close to the shoreline. However, many studies (see for example the Shore Protection Manual, 1984) have shown waves to be strongly reflected seawards of the shoreline due to rapid changes in bathymetry (e.g., a shoal or sand bar). Additionally, laboratory experiments conducted by Guza and Bowen (1976) and Sutherland and O'Donoghue (1997) have shown that there is often a phase change on reflection. Both these factors will lead to an effective reflection line position at a different cross-shore location to that predicted by Eq. (11). It is recommended therefore that the iterative method presented here is used in place of the computationally more efficient Eq. (11) in order to avoid the assumptions that reflection takes place primarily at the shoreline and that there is zero phase shift on reflection. Furthermore, it is not always possible to implement Eq. (11) if the cross-shore profile between the sensor and the shoreline is not accurately known.

---

Fig. 15. (a) An MLM analysis of field data collected in front of a sea wall (Alderney, Channel Islands, UK) on the 7/12/94 at 1853 ( $H_{mo} = 1.14$  m,  $L/S = 0.2$  m). (b) Analysis of the same data file as (a) but using the MMLM with no reflection line position specified. (c) Correlation coefficient (MMLM analysis) and reflection coefficients estimated using the MMLM, MLM and a 2-dimensional analysis method. (d) Estimated reflection line position and theoretical reflection line position given by Eq. (11).

## Acknowledgements

The authors would like to extend their thanks to the Engineering and Physical Sciences Research Council (EPSRC, grant No. GR/H17183) for funding this research programme and to MAST (grant No. MAS2-CT92-0030) for their additional support. We would also like to acknowledge the help from the technicians in the School of Civil and Structural Engineering (Univ. of Plymouth) and all those members of the Plymouth University diving team (Diving and Sailing Centre, Coxside, Plymouth, Devon) who helped with the field deployments.

## References

- Bird, P.A.D., Davidson, M.A., Bullock, G.N., Huntley, D.A., 1994. Wave measurement near reflective structures. Proc. Conf. Coastal Dynamics '94, ASCE, Barcelona, pp. 701–711.
- Davidson, M.A., Bird, P.A.D., Bullock, G.N., Huntley, D.A., 1994. Wave reflection: field measurements, analysis and theoretical developments. Proc. Conf. Coastal Dynamics '94, ASCE, Barcelona, pp. 642–655.
- Davidson, M.A., Bird, P.A.D., Bullock, G.N., Huntley, D.A., 1996. A new non-dimensional number for the analysis of wave reflection from rubble mound breakwaters. Coastal Eng. 28, 93–120.
- Elgar, S., Herbers, T.H.C., Guza, R.T., 1994. Reflection of ocean surface gravity waves from a natural beach. J. Phys. Oceanogr. 24, 1503–1511.
- Forsythe, G.E., Malcolm, M.A., Moler, C.B., 1976. Computer Methods for Mathematical Computations, Prentice-Hall.
- Gautier et al., 1982.
- Gaillard, P., Gauthier, M., Holly, F., 1980. Method of analysis of random wave experiments with reflecting coastal structures. Proc. 17th Conf. on Coastal Eng., ASCE, New York, pp. 204–220.
- Goda, Y., Suzuki, Y., 1976. Estimation of incident and reflected waves in random wave experiments. Proc. 15th Conf. on Coastal Eng., ASCE, New York, pp. 828–865.
- Guza, R.T., Bowen, A.J., 1976. Resonant interactions for waves breaking on a beach. Proc. 15th Conf. on Coastal Eng., ASCE, New York, pp. 560–579.
- Hashimoto, N., Kobune, K., 1987. Estimation of directional wave spectra from a Bayesian approach in incident and reflected wave field. Rep. Port Harbour Res. Inst. 26 (4), 3–33, (in Japanese).
- Huntley, D.A., Simmonds, D.J., Davidson, M.A., 1996. Estimation of frequency dependent reflection coefficients using current and elevation sensors. Proc. Coastal Dynamics, '95. ASCE, New York, NY, pp. 57–68.
- Huntley, Davidson, 1997. Estimation of directional waves near a reflector. Submitted (on 26 July 1996) to Coastal Engineering.
- Isobe, Kondo, K., 1984. Methods for estimating directional wave spectrum in incident and reflected wave field. Proc. 19th Conf. on Coastal Eng., Am. Soc. of Civil Eng., New York, pp. 467–483.
- Mansard, E.P.D., Funke, E.R., 1980. The measurement of incident and reflected spectra using a least squares method. Proc. 17th Conf. on Coastal Eng., ASCE, New York, pp. 154–172.
- Mitsuyasu, H., Tasai, F., Subara, T., Mizuno, S., Okusu, M., Honda, T., Rikiishi, K., 1975. Observations of the directional spectrum of ocean waves using a clover-leaf buoy. J. Phys. Oceanogr. 5, 750–760.
- Nutall, A.H., 1971. Spectral estimation by means of overlapped Fast Fourier Transforms of windowed data, NUSC rep., No. 4169, Dept. of Navy, USA.
- Shore Protection Manual, 1984, US Army Engineer Waterways Experiment Station Coastal Engineering Research Centre.
- Sutherland, O'Donoghue, 1997. Wave phase shift at coastal structures. Paper submitted to: ASCE J. Waterway, Port, Coastal and Ocean Eng.
- Teisson, C., Benoit, M., 1994. Laboratory measurement of oblique irregular wave reflection on rubble mound breakwaters. Proc. 24th Conf. on Coastal Eng., ASCE, New York, pp. 1610–1624.
- Thornton, E.B., Calhoun, R.J., 1972. Spectral resolution of breakwater reflected waves. ASCE J. Waterway, Port, Coastal Ocean Eng. 98 (WW4), 443–460.